World Journal of Nuclear Science and Technology, 2020, 10, 1-8
https://www.scirp.org/journal/wjnst
ISSN Online: 2161-6809
ISSN Print: 2161-6795

Elastic Cross Sections for ^{3}He + ^{58}Ni above the Coulomb Barrier

R. Arceo[1], Omar Pedraza[2], Luis M. Sandoval[1], L. A. López[2], C. Álvarez[1], F. Hueyotl-Zahuantitla[1,3], Ariel Flores-Rosas[1], G. Luis Raya[4], Jesús Martínez-Castro[5]

[1]Facultad de Ciencias en Física y Matemáticas, Universidad Autónoma de Chiapas, Tuxtla Gutiérrez, México
[2]Area Académica de Matemáticas y Física, Universidad Autónoma del Estado de Hidalgo, Pachuca, México
[3]CONACYT, México City, México
[4]Universidad Politécnica de Pachuca, Pachuca, México
[5]Centro de Investigación en Computación, Instituto Politécnico Nacional, México City, México
Email: roberto.arceo@unach.mx, lsandovalm@yahoo.com, crabpulsar@hotmail.com, aros8151@gmail.com, omarp@uaeh.edu.mx, lalopez@uaeh.edu.mx, gilgamesh@upp.edu.mx, macj@cic.ipn.mx, filihz@gmail.com

How to cite this paper: Arceo, R., Pedraza, O., Sandoval, L.M., López, L.A., Álvarez, C., Hueyotl-Zahuantitla, F., Flores-Rosas, A., Raya, G.L. and Martínez-Castro, J. (2020) Elastic Cross Sections for ^{3}He + ^{58}Ni above the Coulomb Barrier. *World Journal of Nuclear Science and Technology*, **10**, 1-8.
https://doi.org/10.4236/wjnst.2020.101001

Received: September 25, 2019
Accepted: November 8, 2019
Published: November 11, 2019

Abstract

In this work, the elastic cross section is calculated at energies above the Coulomb barrier for ^{3}He + ^{58}Ni using a Woods-Saxon potential. The solutions of the radial Schrödinger equations are calculated numerically and they are introduced in the S matrix, after which the cross section is obtained. The parameters in the potential are adjusted to satisfy known experimental data.

Keywords

Elastic and Inelastic Scattering, Scattering Theory, Total Cross Sections

1. Introduction

We have studied the scattering of nuclei by helium and nickel atoms using the Schrödinger equation at energies up to 35 MeV for the reaction ^{3}He + ^{58}Ni using a radial Woods-Saxon potential. We treated the Schrödinger equation numerically, for the case of the *Woods-Saxon* potential [1]; the parameters for this potential were adjusted to coincide with known experimental data.

The value of chi-squared was minimized by using a theoretical model and the experimental data from Fujisawa *et al.* [2]. The parameters thus obtained are used in the Woods-Saxon potential and we compare the results with known experimental data.

Recently we have results at low energies for the reaction $^{3,4,6}He$ + ^{58}Ni [2] [3] [4] [5]. We compare our results for this reaction and show that the Woods-Saxon potential agrees with known experimental data.

This paper is divided into four sections as follows. In Section 2, we briefly describe the setup; Section 2.1 is dedicated to obtaining the Woods-Saxon potential. In Section 2.2, we discuss the elastic cross section for the scattering of helium by nickel atoms. In Section 3, the obtained results are shown. Finally, in Section 4 we focus on the discussion of our results.

2. Theory

In this section we describe the procedure used to compute the Woods-Saxon potential produced by a point particle. We then calculate the cross section for the collision of two particles of mass $m_{1,2}$ and atomic number $Z_{1,2}$. Our approach to this problem is numerical, and we make the assumption that the interaction of the incident particle with the rest atom can be accounted for by the effective Woods-Saxon potential which we calculate below. We minimize the value of chi squared from the experimental ^{3}He + ^{58}Ni data [2] and the parameters we obtain are shown in **Table 1** and **Table 2**.

2.1. The Woods-Saxon Potential

The Woods-Saxon potential is a mean field potential for the nucleons (protons and neutrons) inside the atomic nucleus, which is used to describe approximately the forces applied on each nucleon, in the nuclear shell model for the structure of the nucleus.

The standard Woods-Saxon potential [1], as a function of the distance r^* from the nuclear center, is defined by:

$$V'\left(r^*\right) = -\frac{V_0}{1+\exp\left(\frac{r^*-R}{a}\right)}, a \ll R \tag{1}$$

Table 1. Parameters obtained for the reaction ^{3}He + ^{58}Ni.

E	l	V_0	R_1	a_1	W_0	R_2	a_2	σ_R	σ_T	χ^2/N
(MeV)	up to	(MeV)	(fm)	(fm)	(MeV)	(fm)	(fm)	(mb)	(mb)	
24.15	11	174.400	1.30	0.750	17.1	1.41	0.71	1476.904	2871.663	11.95
27.64	15	174.275	0.93	0.601	17.1	1.41	0.71	1526.071	3542.422	5.85
34.14	13	174.500	0.94	0.75	18.6	1.41	0.73	1620.872	2695.711	2.21

Table 2. Parameters obtained with the derivative in the complex term of the Woods-Saxon potential for the reaction ^{3}He + ^{58}Ni.

E	l	V_0	R_1	a_1	W_0	R_2	a_2	σ_T	χ^2/N
(MeV)	up to	(MeV)	(fm)	(fm)	(MeV)	(fm)	(fm)	(mb)	
24.15	11	175.0	1.3	0.75	18.2	1.41	0.72	3277.768	17.903
27.64	15	173.6	1.3	0.75	17.1	1.41	0.71	3046.658	5.047
34.14	13	173.9	0.94	0.75	18.9	1.41	0.73	2804.289	1.832

where V_0 (with dimensions of energy, MeV) represents the potential well depth, *a* is a length representing the "surface thickness" of the nucleus, and $R = r_0 A^{1/3}$ is the nuclear radius where $r_0 = 1.25\ \text{fm}$ and A is the atomic mass number.

It is interesting to examine the consequences of the radial effective Woods-Saxon potential, $V_{WS}\left(r^*\right)$, by using both real and imaginary terms in experiments such as scattering events. We do so in the following section, where we include the Coulomb interaction potential $V_C\left(r\right)$. The total radial effective potential used is

$$V\left(r\right) = V_C\left(r\right) + V_{WS}\left(r^*\right), \tag{2}$$

$$V\left(r\right) = \frac{1.44 Z_{1,2}}{r} - \frac{V_0}{1+\exp\left(\frac{r^*-R_1}{a_1}\right)} - \frac{iW_0}{1+\exp\left(\frac{r^*-R_2}{a_2}\right)}. \tag{3}$$

In Figure 1, we show the real and imaginary parts of the Woods-Saxon potential.

2.2. The Schrödinger Equation with the Woods-Saxon Potential

In this section we solve the radial Schrödinger equation using the radial potential (Equation (3)). The Schrödinger equation is,

$$\left[-\frac{\hbar^2}{2\mu}\nabla^2 + V\left(r\right)\right]\Psi\left(\boldsymbol{r}\right) = E\Psi\left(\boldsymbol{r}\right), \tag{4}$$

where $\mu = \frac{m_1 m_2}{m_1 + m_2}$ is the reduced mass for a two-particle system, E is the energy and $V\left(r\right)$ is the radial effective potential calculated in the previous section.

We introduce $U\left(r\right)$, where

$$\Psi\left(\boldsymbol{r}\right) = \Psi\left(r\right) = \frac{U\left(r\right)}{r}, \tag{5}$$

and the Schrödinger Equation (4) is solved by the method of separation of variables. For the radial component we obtain

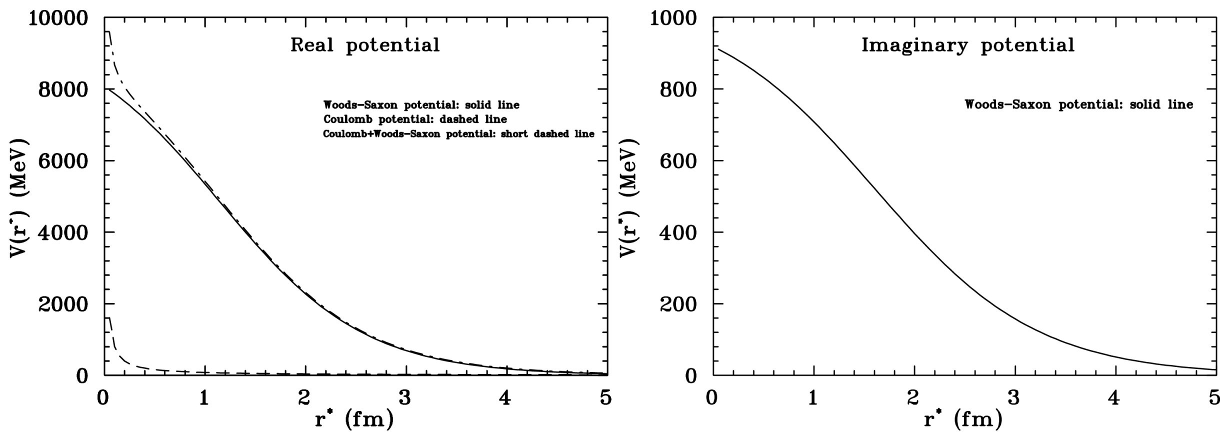

Figure 1. The solid line is for the Woods-Saxon potential using the parameters obtained from the Colorado group (Table I-a from Ref. [2]) and the dashed line is for the Coulomb potential.

$$U_l''(r)+\frac{2\mu}{\hbar^2}\left[E-V(r)\right]U_l(r)-\frac{l(l+1)}{r^2}U_l(r)=0. \tag{6}$$

The radial equation takes the final form,

$$U_l''(r)+\frac{2\mu}{\hbar^2}\left[E-\frac{1.44Z_{1,2}}{r}+\frac{V_0}{1+\exp\left(\frac{r^*-R_1}{a_1}\right)}+\frac{iW_0}{1+\exp\left(\frac{r^*-R_2}{a_2}\right)}\right]U_l(r) \tag{7}$$
$$-\frac{l(l+1)}{r^2}U_l(r)=0.$$

The next step is to determine the set of the parameters for the Woods-Saxon potential. In the **Table 1** and **Table 2** we show the parameters obtained by minimizing the chi squared value,

$$\chi^2=\sum_{i=1}^{N}\left[\frac{\sigma_{th}(\theta_i)-\sigma_{exp}(\theta_i)}{\Delta\sigma_{exp}(\theta_i)}\right]^2. \tag{8}$$

The calculations for this analysis were done using the experimental data from Fujisawa *et al.* [2].

In **Table 1** and **Table 2** we show the parameters obtained by minimizing chi squared and using the experimental data from Fujisawa *et al.* [2].

The numerical techniques necessary to solve the Schrödinger equation with a radial potential are explained in chapter 3, Equation (3.28) of Ref. [6]. The solutions of U_l from Equation (7) are introduced in the S matrix (Eq. 10.58 of Ref. [6]), which is,

$$S_l=\frac{U_l(r_{n-1})r_n h_l^-(kr_n)-U_l(r_n)r_{n-1}h_l^-(kr_{n-1})}{U_l(r_n)r_{n-1}h_l^+(kr_{n-1})-U_l(r_{n-1})r_n h_l^+(kr_n)}, \tag{9}$$

where the S matrix is evaluated in the last two points on a mesh of size δ ($r=0,\delta,2\delta,\cdots,n\delta$). U_l are the solutions to the Schrödinger equation with the potential previously calculated and h_l are the spherical Hankel functions defined in Eq. 10.52 of Ref. [6]. The scattering amplitude for a *partial wave decomposition* in terms of the S matrix is,

$$f(\theta)=\frac{1}{2ik}\sum_{l=0}^{\infty}(2l+1)P_l(\cos\theta)(S_l-1). \tag{10}$$

For states with well defined spin and isospin the elastic and total cross section of nucleon-nucleon scattering into a solid angle element $\mathrm{d}\Omega$ is given by the scattering amplitude $f(\theta)$ of the reaction

$$\frac{\mathrm{d}\sigma}{\mathrm{d}\Omega}=\left|f(\theta)\right|^2, \tag{11}$$

$$\sigma_T=\frac{4\pi}{k}Im\left[f(0^\circ)\right], \tag{12}$$

where k is the center-of-mass momentum and $f(0^\circ)$ is the forward amplitude.

The reaction cross section is defined as the subtraction from the integral of the elastic cross section from the total cross section,

$$\sigma_R \equiv \frac{2\pi}{k^2}\sum_{\ell=0}^{\infty}(2\ell+1)Re(1-S_\ell)-\int\sigma(\theta)\mathrm{d}\Omega. \tag{13}$$

Doing the integration gives

$$\sigma_R = \frac{2\pi}{k^2}\sum_{\ell=0}^{\infty}(2\ell+1)Re(1-S_\ell)-\frac{\pi}{k^2}\sum_{\ell=0}^{\infty}(2\ell+1)\left[|S_\ell|^2+1-2ReS_\ell\right], \tag{14}$$

$$\sigma_R = \frac{\pi}{k^2}\sum_{\ell=0}^{\infty}(2\ell+1)\left(1-|S_\ell|^2\right). \tag{15}$$

The results from the calculations are shown in the next section.

3. Elastic Cross Section

With the analysis performed, we proceed to evaluate numerically the Equations (11)-(12) and (15). We compare the theoretical results with experimental data for elastic cross sections for elastic scattering of helium by nickel atoms [2]. This comparison is made explicitly in **Figures 2-5**.

In **Figures 2-4** the elastic cross section is analyzed for helium by nickel atoms. We evaluate the elastic cross section at energies from T_{Lab} = 24.15, 27.64 and 34.14 MeV considering the radial effective Woods-Saxon potential and setting the parameters to adjust the experimental points (see **Table 1** and **Table 2**).

In **Figure 5** we show the differential cross section at energies above the Coulomb barrier.

Figure 6 shows the total and reaction cross section for the interaction of helium by nickel atoms. We evaluate the cross sections at energies up to $T_{Lab} = 35\ \mathrm{MeV}$ considering the radial effective Woods-Saxon potential and setting the parameters to adjust the experimental points (see **Table 1**).

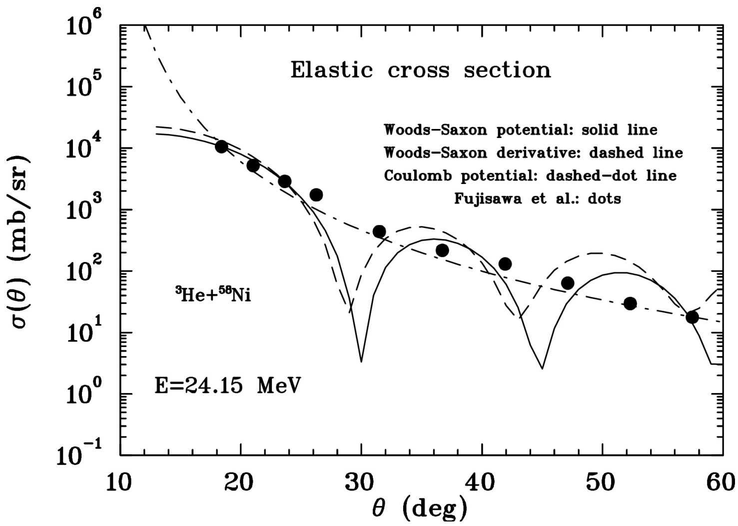

Figure 2. The differential cross section for ^{3}He + ^{58}Ni is plotted as a function of the angle at the energy of 24.15 MeV. The solid line is for the Woods-Saxon potential, the dashed line is with the derivative in the complex term for the Woods-Saxon potential, and the dashed-dot line is for the Coulomb potential. The experimental points come from [2].

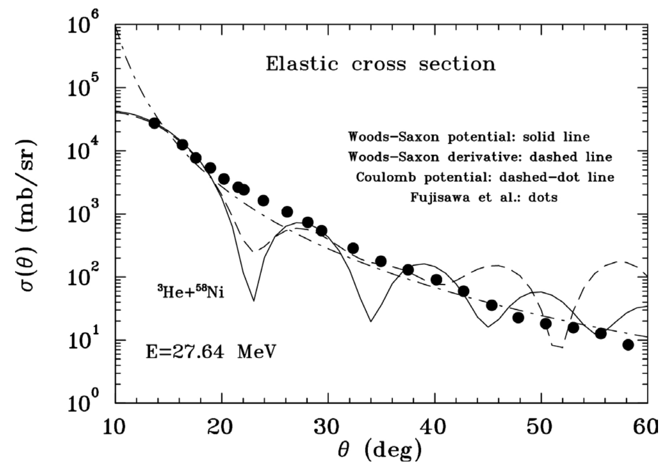

Figure 3. The differential cross section for ^3He + ^{58}Ni is plotted as a function of the angle at the energy of 27.64 MeV. The lines and the experimental points have the same meaning as in **Figure 2**.

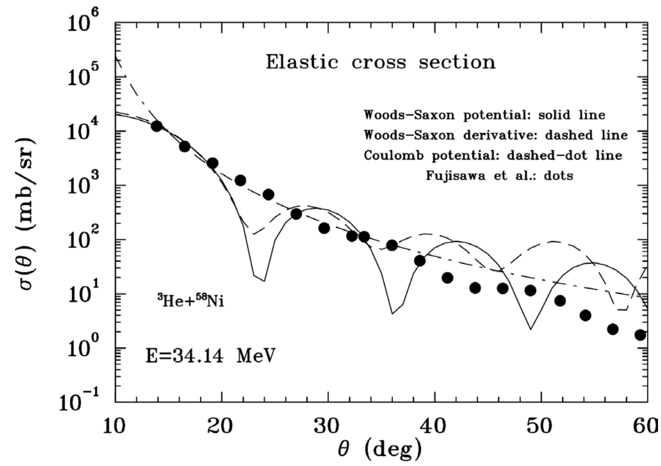

Figure 4. The differential cross section for ^3He + ^{58}Ni is plotted as a function of the angle at the energy of 34.14 MeV. The lines and the experimental points have the same meaning as in **Figure 2**.

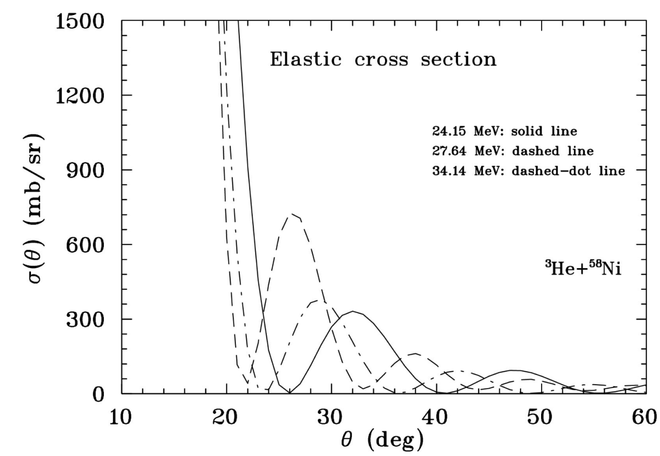

Figure 5. ^3He + ^{58}Ni elastic scattering for energies at the barrier Coulomb plotted as a function of the angular distribution. The lines are for the case of a Woods-Saxon potential.

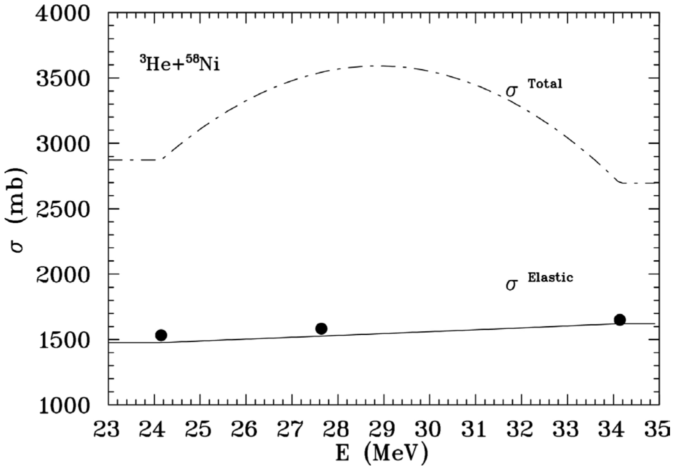

Figure 6. The total and integrated elastic scattering cross section for ^{3}He + ^{58}Ni are plotted as a function of the incident energy. The experimental points come from [2].

4. Conclusions

In this work, we present a numerical solution of the radial Schrödinger equation using a Woods-Saxon potential. We have examined the scattering of helium atoms via nickel. The scattered from alpha particles via nickel atoms was performed and the use of an imaginary term in the Woods-Saxon potential gives a better fit to the experimental data. The parameters for the Woods-Saxon potential were varied until χ^2 was minimized and they are shown in **Table 1** and **Table 2**. The values obtained are better in comparison to those of the Colorado group (Table I-a from Ref. [2]) at the energies of 24.15, 27.64 and 34.14 MeV.

Finally, the total cross section and integrated elastic scattering cross section are calculated and compared with experimental data. We obtain excellent agreement with the experimental data of Fujisawa *et al.* (Ref. [2]) for the set of parameters obtained in **Table 1** and **Table 2**.

Acknowledgements

This work was partially supported by FCFM-UNACH. R. Arceo acknowledges the support of the PFCE 2018.

Conflicts of Interest

The authors declare no conflicts of interest regarding the publication of this paper.

References

[1] Woods, R.D. and Saxon, D.S. (1954) Diffuse Surface Optical Model for Nucleon-Nuclei Scattering. *Physical Review*, **95**, 577-578.
https://doi.org/10.1103/PhysRev.95.577

[2] Fujisawa, T., Kamitsubo, H., Wada, T. and Igarashi, M. (1969) Optical-Model Analysis of Elastic Scattering of ^{3}He Particles from ^{58}Ni at 24.15, 27.64 and 34.14 MeV. *Journal of the Physical Society of Japan*, **27**, 278-290.

https://doi.org/10.1143/JPSJ.27.278

[3] Jansen, R.H.J., de Heer, F.J., Luyken, H.J., van Wingerden, B. and Blaauw, H.J. (1976) Absolute Differential Cross Sections for Elastic Scattering of Electrons by Helium, Neon, Argon and Molecular Nitrogen. *Journal of Physics B*, **9**, 185-212. https://doi.org/10.1088/0022-3700/9/2/009

[4] Baron, N., Leonard, R.F. and Stewart, W.M. (1971) Alpha-Gamma Angular Correlations in ^{12}C, ^{24}Mg, ^{58}Ni, and ^{120}Sn. *Physical Review C*, **4**, 1159-1173. https://doi.org/10.1103/PhysRevC.4.1159

[5] Albinski, J., Budzanowski, A., Dabrowski, H., Rogalska, Z., Wiktor, S., Rebel, H., Srivastava, D.K., Alderliesten, C., Bojowald, J., Oelert, W., Mayer-Böricke, C. and Turek, P. (1985) α-Particle Scattering from Ni Isotopes at $E_\alpha = 172.5$ MeV. *Nuclear Physics A*, **445**, 477-494. https://doi.org/10.1016/0375-9474(85)90453-1

[6] Gibbs, W.R. (2006) Computation in Modern Physics. 3rd Edition, World Scientific Publishing, Singapore.